Chin. J. Astron. Astrophys. Vol. 3 (2003), No. 5, 469–477
(http://www.chjaa.org or http://chjaa.bao.ac.cn)

Chinese Journal of Astronomy and Astrophysics

An Analysis of Average Pulsar Profiles and A Study of the ρ-P relation of Pulsars *

Hua-Xiang Wang and Xin-Ji Wu

Department of Astronomy, Peking University, Beijing 100871; wuxj@vega.bac.pku.edu.cn
Urumqi Astronomical Station, National Astronomical Observation, Urumqi 830011
CAS-PKU Joint Beijing Astrophysics Center, Beijing 100871

Received 2003 March 21; accepted 2003 May 14

Abstract Using the method of Gaussian Fit Separation of Average Profile (GFSAP), we re-examine the average profiles of nine pulsars at several frequencies, ranging from 408–1642 MHz. This method enables us to obtain the number of components for each pulsar, and the parameters for each component, the width, position and amplitude. The ρ-P relation for the inner cone and outer cone are studied separately, and the results are, respectively, $\rho = P^{-0.51\pm0.05}$ and $\rho = P^{-0.42\pm0.06}$. The results can be interpreted as a confirmation of the double-cone structure of pulsar emission beams. The altitudes of emission region, and the radius-to-frequency-map (RFM) are also examined; for the outer cone, we obtained $r(\nu) \propto \nu^{-0.19\pm0.09}$.

Key words: stars: pulsar: general — line: profiles

1 INTRODUCTION

The mean pulse profile of pulsars has been considered as an important tool for understanding the pulsar phenomenon, including the geometry of the pulsar emission beams, polarization behavior. In some way, the geometry of pulsar emission beams has provided important insight into the mechanism of pulsar radiation. Many authors have studied the structure of pulsar emission beams. First the hollow-cone model was suggested (Radhakrishnan & Cooke 1969; Komesaroff 1970); then, in order to explain triple type profiles, Backer (1976) introduced the central pencil-beam emission near the magnetic axis; Lyne & Manchester (1988, hereafter LM88) concluded that the emission is randomly distributed within an almost circular region, which can be called "window function". Rankin established an empirical theory of pulsar emission, and introduced a comprehensive pulsar classification scheme. In the papers (Rankin 1993a, b, hereafter R93a, b), a special consideration was given to the five-component (M) class, and their two pairs of conal components suggest the emission from two hollow cones, an inner cone and an outer cone. Moreover, the five-component profile represents a central traverse of

* Supported by the National Natural Science Foundation of China.

the sight line through the two concentric conal emission zones and a core beam, can reflect the full phenomenological potential of the emission process, and also provide a most comprehensive understanding of the geometry of the beam structure. However, rather few pulsars have been identified as of the five-component type. On the one hand, the "boxy", squarish shape caused by conal narrowing at high frequency, makes it difficult to identify the individual components. On the other hand, the empirical analyses may sometimes introduce uncertainties in the results.

To improve on these deficiencies, average pulsar profiles are often separated into individual components using different methods. The assumption that a single pulse components in pulsar profiles can be best represented by a Gaussian has been proposed by several authors (Krishnanmohan & Downs 1987; Wu et al. 1992a, b), so a given profile was separated into individual components by fitting it with a sum of Gaussians. Wu et al. (1992a, 1998) developed a method of Gaussian fit separation of the average profile (GFSAP) to explore the latters detailed structure, in which the total profile is modeled as a superposition of several Gaussian-shaped components. They applied this method to the pulsar PSR B1451–68, and obtained a good result on the geometrical properties of the three distinct emission zones, the core, the inner and outer cone, and on the spectrum of each zone. This method has been used to analyze the pulse profiles of pulsars by other authors (Kramer et al. 1994, 1996; Kuzmin et al. 1996; Xu et al. 2002).

There are always contentions on the relation between the opening angle ρ and the period P. In the early period Gunn & Ostriker (1970) gave the relation $\rho \propto P^{-0.5}$, which was supported by several results (Kuzmin et al. 1984, 1992; Wu et al. 1995). However, relations with different values of the exponent, $\rho \propto P^{-0.67}$ and $\rho \propto P^{-0.33}$, have been put forward by Ruderman et al. (1975) and LM88. The ρ-P relation of the inner and outer cones were studied in R93a. A difficulty here is how to extract the apparent width of the inner cone from the observations, and the GFSAP provides an effective approach to this problem.

Table 1 List of Studied Pulsars

PSR B	Period (s)	α (deg)	β (deg)	Classified by Rankin	Our Result
0402+61	0.594574	83.0	2.2	M	five (M)
0450–18	0.548938	24.0	4.0 $^{\rm LM}$	T	three (T)
1039–19	1.386368	31.0	1.7	M	four (cQ)
1237+25	1.382449	53.0	0.0	M	five (M)
1737+13	0.803050	41.0	1.9	M	five (M)
1804–18	0.163727	63.0	5.1	M/T	three (T)
1831–04	0.290106	10.0	2.0	M	five (M)
1857–26	0.612209	25.0	2.2	M	five (M)
2310+42	0.349434	56.0	6.8	M	four (cQ)

Here LM means the value is from LM88. The symbol M in the table represents the multi-component (particularly five-component) type, T means triple type with cone, St means single-core type, and cQ means conal quadruple type. Our fitted components follow the class scheme.

In this paper, we applied the GFSAP method (cf. Sect. 2) to the profiles of nine pulsars. This method allows us a refined study of the pulsar's emitting geometry. The data set is from the polarimetric observations of 300 pulsars with the 76-m Lovell Telescope at Jodrell Bank (Gould et al. 1998) at radio frequencies centered around 230, 408, 610, 925, 1408, 1642 MHz. We adopted the data from 408–1642 MHz, as the basis for a multi-frequency analysis. In order to obtain reliable results, we picked out pulsars with good profiles, i.e. where the noise level

is relatively small, and the average profile has better S/N ratios. Furthermore, pulsars with "complex" profiles were preferred, especially those characterized by five components, for their more complex geometry deserves particular attention. The pulsars we studied here are listed in Table 1. In Sect. 2, we briefly describe the GFSAP method by means of which we can obtain, for each pulsar, the number of components and the parameters for each component, the width, position, and amplitude. The results are presented in Sect. 3. In Sect. 4 the ρ-P relation for the inner cone and outer cones are studied separately. The altitudes of the emission region, and the radius-frequency-map (RFM) are then examined in Sect. 5.

2 THE GSFAP METHOD

The key factor in the analysis of complex pulse profiles is the correct number of real components. Our analytic profile model is based on the assumption that the average profile of a component has a Gaussian form. First we assume a small number of components and then add others until a satisfactory fit is achieved. In general, the total profile $f(\phi)$ (ϕ is the phase of the average profile, expressed in degrees) can be written as the sum of a small number M of Gaussian components,

$$f(\phi) = \sum_{j=1}^{M} g_j, \tag{1}$$

where

$$g_j = h_j e^{-4ln2(\phi - p_j)^2/w_j^2}, \tag{2}$$

in which the j-th component g_j has amplitude h_j, peak phase p_j and half-power width w_j. The residuals of any model curve that successfully fits the observations should be comparable to the observational errors. The sum of squared residuals is

$$Q = \sum_{i=1}^{N} (f(\phi)_i - y(\phi)_i)^2 = \sum_{i=1}^{N} \{[\sum_{j=1}^{M} g(\phi)_j]_i - y(\phi)_i\}^2. \tag{3}$$

Here $y(\phi)_i$ is the observed value at data point labeled i, $(i = 1, 2, \cdots, N)$, N being the total number of data points considered. The values of p_j, h_j, and w_j $(j = 1, 2, \cdots, M)$ are determined by minimizing the quantity Q. By considering both the polarization structure and overall frequency evolution of the profile, the fitted results can be improved by making careful reference to the observational data by choosing better initial parameters. The rms amplitude is given by

$$\sqrt{Q/N} = \sqrt{\{\sum_{i=1}^{N} (f(\phi)_i - y(\phi)_i)^2\}/N}. \tag{4}$$

Our fitting procedure can be described as follows:

1) Define the on-pulse and off-pulse region. First, find the position where the flux reaches 10% of the maximum flux. Extend it 10 degree left-and-right, and we have the "on-pulse" region. The region outside the on-pulse region is the "off-pulse" region. We estimate the initial parameters of fitting, by assuming the small number of components that can be obviously identified from the observed profiles and polarization data.

2) The fitting program is applied to the data, and the mean residual is calculated.

3) Compare the mean residual to the rms of the off-pulse regions. If the difference is more than 3σ of the off-pulse region, then we add a new component, possibly centered at the largest peak of the post-fit residuals.

4) Repeat steps 2) and 3) until the distribution of the residuals is as same as those in the off-pulse regions.

3 FITTED PROFILES AND THE CLASSIFICATIONS

Most of the pulsars we selected are classified as M-type (R93a) in Rankin's scheme of classification. Since the empirical method used by R93a might induce some uncertainties, we re-examined the profiles in the light of our more accurate fitting procedure. Our results are given in the last column of Table 1, following the basic parameters and the Rankin classification.

From the fitting procedure, we acquire for each pulsar, the number of components and the parameters for each component. There are two pulsars (PSR1309–19 and 2310+42) with four components, which is different from the classification given by R93a.

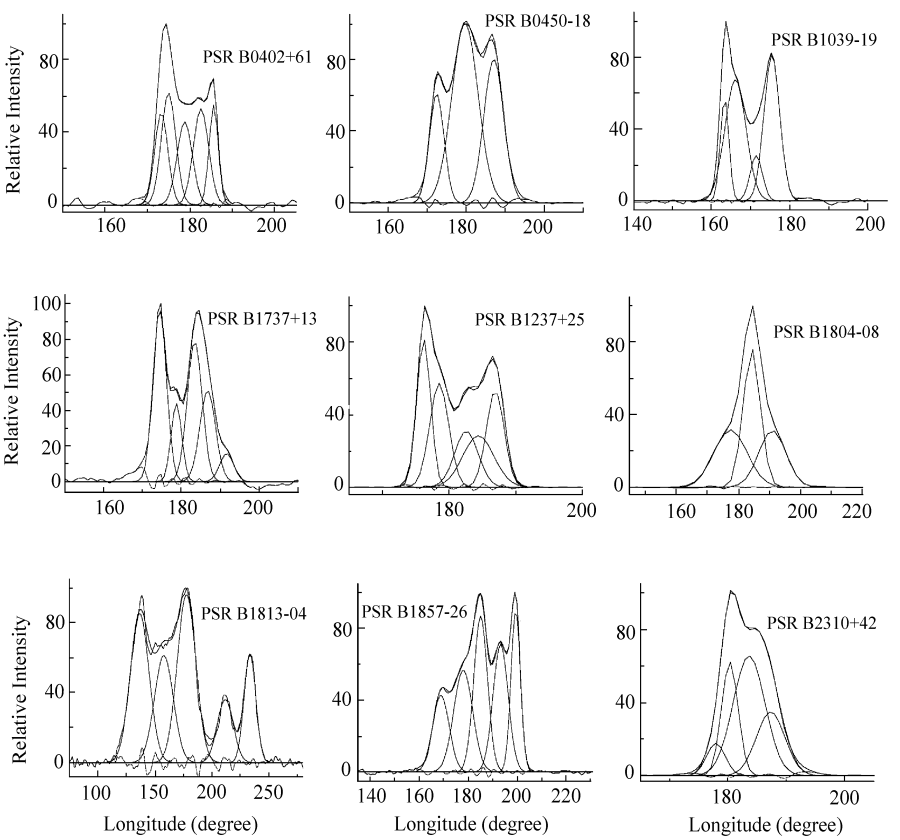

Fig. 1 Profiles of nine pulsars at 610 MHz. Abscissa is pulse phase in degrees and ordinate is pulse amplitude in arbitrary units. Solid lines represent the observed average profiles, dashed line, the fitting curves, and dotted-dash lines, the residual curves.

Figure 1 shows the pulsar profiles at the frequency of 610 MHz, each superposed with the individual Gaussian components and their sum (the fitting curve), and the residual curve. The fitting curves reproduce the original profiles quite well within the observational uncertainties. Although the S/N ratio is not good for part of the data, e.g., PSR B1737+13 at some frequencies; PSR B1831-04 at all frequencies, thus affecting the accuracy of the fitting, the residuals appear to have a pure noise character, in contrast to the systematic trends seen in the fitting curves. This confirms that the fitting is reasonable and acceptable.

The classification of the pulsars is important for our further analysis and should be noted carefully;—particularly the number of components given by the fitting procedure.

4 THE ρ-P RELATIONS FOR THE INNER AND OUTER CONES

The opening angle ρ between the magnetic axis and the emission direction is given in G81 and R93a as

$$\rho = \cos^{-1}[\cos\beta - 2\sin\alpha\sin\zeta\sin^2(\Delta\phi/4)], \tag{5}$$

where α is the inclination angle (i.e. the angle between the magnetic axis and the spin axis), β is the the angle between the line-of-sight and the magnetic axis, ζ is the angle between the line-of-sight and the rotation axes, and $\Delta\phi$ is the half power width of the pair of conal components (either inner or outer cone). The fitted results of the half power width ($\Delta\phi$) and the calculated values of the opening angle (ρ) for nine pulsars at five frequencies listed in Table 2.

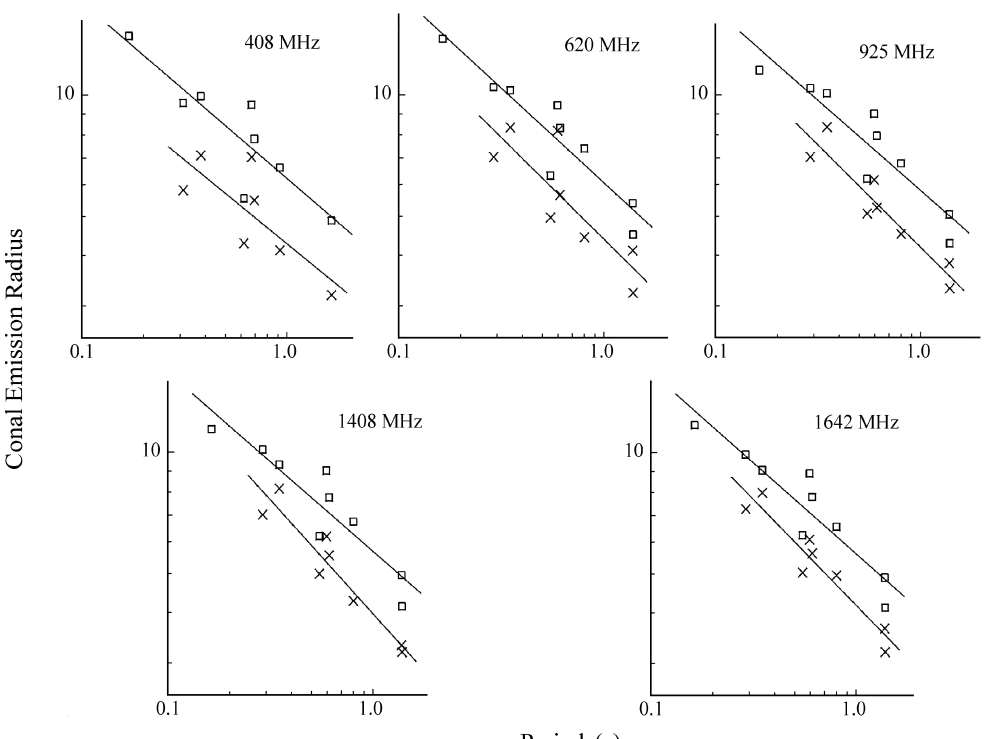

Fig. 2 Plot of the opening angle ρ for the inner and outer emission cone at five frequencies. Crosses represent the inner component, and boxes, the outer components. The best-fit lines are also shown for the two groups of points.

Table 2 Emission Geometry of Nine Pulsars

		Inner		Outer		r (km)	
PSR B	Freq (MHz)	$\delta\phi$	ρ	$\delta\phi$	ρ	inner	outer
0402+61	408	15.2	7.9	20.4	10.4	368.4	645.5
	610	15.8	8.2	18.5	9.5	397.1	531.1
	925	11.6	6.2	17.6	9.0	228.4	484.1
	1408	11.7	6.2	17.6	9.0	225.8	482.1
	1642	11.4	6.1	17.3	8.9	220.3	469.6
0450-18	408	20.0	5.9	—	—	192.9	—
	610	19.9	5.9	—	—	191.5	—
	925	19.6	5.86	—	—	188.7	—
	1408	19.6	5.86	—	—	188.6	—
	1642	19.5	5.84	—	—	187.1	—
1039-19	610	10.4	3.2	15.8	4.8	166.3	326.0
	925	10.8	3.3	14.9	4.3	151.8	254.7
	1408	10.3	3.2	14.3	4.1	141.5	238.2
	1642	10.2	3.2	14.2	4.1	141.3	235.3
1237+25	408	9.4	3.8	14.0	5.6	195.9	433.6
	610	10.3	4.1	13.5	5.4	233.7	401.9
	925	9.6	3.8	12.7	5.1	202.4	353.5
	1408	8.3	3.3	12.4	5.0	152.6	340.7
	1642	9.1	3.6	12.4	4.9	183.7	338.2
1737+13	408	13.1	4.8	21.5	7.4	183.7	444.1
	610	12.0	4.7	21.3	7.6	179.7	459.3
	925	12.3	4.8	19.5	6.8	164.1	368.8
	1408	11.5	4.3	19.4	6.7	147.0	364.8
	1642	13.7	4.9	18.7	6.5	197.0	343.3
1804-08	408	—	31.1	—	15.0	—	246.6
	610	—	28.2	—	13.8	—	208.5
	925	—	22.8	—	11.5	—	145.4
	1408	—	22.5	—	11.4	—	142.9
	1642	—	23.2	—	11.7	—	149.5
1831-04	408	67.1	6.6	112.9	10.5	126.3	320.3
	610	72.0	7.0	112.6	10.5	143.1	318.6
	925	72.0	7.0	111.8	10.4	143.3	314.7
	1408	71.9	7.0	109.1	10.2	142.6	301.1
	1642	74.5	7.2	105.6	9.9	152.0	284.1
1857-26	408	24.5	5.8	37.9	8.6	205.9	451.4
	610	23.4	5.6	36.7	8.3	190.7	424.7
	925	21.8	5.3	34.8	7.9	169.3	385.4
	1408	23.3	5.6	33.9	7.7	189.2	366.9
	1642	21.0	5.1	33.4	7.6	159.3	358.6
2310+42	408	9.6	8.0	19.8	10.9	220.9	415.3
	610	8.2	7.7	14.1	9.1	204.7	290.8
	925	8.7	7.8	14.1	9.1	210.2	289.0
	1408	8.5	7.7	14.1	9.1	208.7	289.8
	1642	8.0	7.6	13.5	8.9	202.5	280.1

Several authors have studied the opening angle ρ of the conal components and the ρ-P relation in the form, $\rho = AP^{-\sigma}$, containing the all-important exponent σ. Now we turn to analysis the ρ-P relation. Figure 2 plots the relation for the inner and outer cones at the five frequencies. The numerical data are given in Table 3.

Now we can make a comparison of our results with other authors'. At 920 MHz, our results are:

$$\rho_{\rm inner} = (4.17^\circ \pm 0.19^\circ)P^{-0.51\pm0.07}, \tag{6}$$

and

$$\rho_{\rm outer} = (5.81^\circ \pm 0.40^\circ)P^{-0.45\pm0.07}\,. \tag{7}$$

These results are consistent with Rankin's results at 1.0 GHz, $4.33^\circ P^{-0.52}$ for the inner cone and $5.75^\circ P^{-0.50}$ for the outer cone, as well as the results of Gil et al. (1993), $(4.15^\circ \pm 0.5^\circ)P^{-0.46\pm0.05}$ and $(5.52^\circ \pm 0.5^\circ)P^{-0.49\pm0.02}$ for the two cones. The ρ value versus period reveals a binomial distribution, showing that the double cone structure proposed by R93a can be used to explain the observational profiles of most pulsars. Considering the exponents at all five frequencies, we obtain an average exponent $\bar{\sigma}$ of 0.51 ± 0.10 for the inner cone, and 0.45 ± 0.07 for the outer. The inner cone exponent agrees with the value –0.52 of R93a very well, while for the outer one, our result is somewhat lower.

Table 3 Linear Fitting Results of the ρ-P Plot at Five Frequencies

	$\rho_{\rm inner} = AP^{-\sigma}$		$\rho_{\rm outer} = BP^{-\sigma}$	
Frequency (MHz)	A (deg)	σ	B (deg)	σ
408	4.68±0.54	0.42±0.15	6.61±0.61	0.44±0.09
610	4.37±0.40	0.51±0.13	6.03±0.42	0.47±0.07
925	4.17±0.19	0.51±0.07	5.81±0.40	0.45±0.07
1408	3.98±0.39	0.57±0.7	5.69±0.39	0.45±0.07
1642	4.16±0.18	0.53±0.07	5.61±0.39	0.45±0.07

5 ALTITUDE OF THE EMISSION REGION OF THE OUTER CONE COMPONENT

Table 4 shows the calculated values of the altitude of the emission region of the outer cone component for the pulsars. The two "r"s in the table represent the emission heights of the two cones above the neutron star center, on the assumption that these radiation zones are bounded by the last open field lines and that the star has a 10 km radius, following Gil (1981) and R93a:

$$r(\mathrm{km}) = 6.66\rho^2 P. \tag{8}$$

Table 4 Results for Radius-to-Frequency Mapping

	$R_{\rm inner} = A\nu^{-p}$		$R_{\rm outer} = B\nu^{-p}$	
PSR B	A(km)	p	B(km)	p
0402+61	263.6±18.2	0.44±0.14	501.2±11.7	0.21±0.05
0450–18	138.0±1.0	–0.02±0.01	213.8±1.0	0.02±0.01
1039–19	144.5±2.7	0.04±0.05	257.0±1.8	0.18±0.02
1237+25	186.7±12.9	0.16±0.12	363.2±8.4	0.20±0.02
1737+13	169.8±11.7	0.01±0.12	380.2±7.1	0.19±0.03
1804–08	—	—	251.2±11.6	0.40±0.10
1831–04	144.6±3.1	–0.10±0.04	302.0±4.2	0.08±0.02
1857–26	190.5±8.8	0.14±0.07	389.0±4.5	0.16±0.02
2310+42	229.1±5.3	0.01±0.05	331.1±5.4	0.26±0.3

The calculated values of the altitude of emission region (r) for nine pulsars at five frequencies listed in Table 2. Various methods have been used to estimate the emission altitudes. These estimates show that the pulsar emission region is relatively narrow and lies near the surface of the neutron star, apparently closer than about 10 percent of the light cylinder radius (at least for normal pulsars). Now it is widely believed that the emission mechanism is narrow-band

and different frequencies are produced at different altitudes above the magnetic polar cap. This concept is known as radius-to-frequency mapping (RFM), that is,

$$r_{\rm em} \propto \nu^{-p}. \tag{9}$$

As we can see, for the inner cone, the emission altitude changes little over the five frequencies. For the outer cone, an average exponent $\bar{p}$ can be obtained, $\bar{p} = 0.19 \pm 0.04$; this value is consistent with the estimates in other papers (KG97, KG98, Wu99, and Wu02).

6 CONCLUSIONS

Applying the GFSAP method to nine pulsars, we have decomposed their average profiles each into several components. The fitting results reconstruct the original profiles very well within the statistical errors of the observation. A careful geometrical analysis of the fitting results clearly reveals that the pulsar emission beam has a double-cone structure.

The emission opening angle at 50% level of the maximal flux intensity, ρ, varies as $P^{-0.51\pm0.05}$ and as $P^{-0.42\pm0.06}$, for the inner and outer cone, respectively. The value of the exponent of the inner cone accords very well with R93a's value (–0.52) while that for the outer cone is rather smaller than that of R93a. Our results fully support the model of double cone-core beam structure of R93a, b.

We found that the altitude of the inner cone emission region $r_{\rm em}^{\rm inner}$ is generally $< 250\,{\rm km}$, and the outer cone $r_{\rm em}^{\rm outer} < 500\,{\rm km}$. The emission altitude of the inner cone changes little with frequencies, whereas for the outer cone, we obtained a radius to frequency mapping of $r(\nu) \propto \nu^{-0.19\pm0.09}$, consistent with the results of other authors.

Acknowledgements This work was supported by National Natural Science Foundation of China under Grant 10073001 and 10173021.

References

Backer D. C., 1976, ApJ, 209, 895
Gil J. A., 1981, A&A, 104, 69
Gil J. A., Kijak J., Sciradakis J. H., 1993, A&A, 272, 268
Gould D. M., Lyne A. G., 1998, MNRAS, 301, 235
Gunn J. E., Ostriker J. P., 1970, ApJ, 160, 979
Kijak J., Gil J., 1997, MNRAS, 288, 631 (KG97)
Kijak J., Gil J., 1998, MNRAS, 299, 855 (KG98)
Krishnamohan S., Downs G. S., 1983, ApJ, 265, 372
Komesaroff M. M., 1970, Nature, 225, 612
Kramer M., Wielebinski R., Jessner A. et al., 1994, A&AS, 515, 526 (Kramer et al. 94)
Kramer M., Xilouris K. M., Jessner A. et al., 1996, A&A, 306, 867
Kuzmin A. D., Wu X. J., 1992, Ap&SS, 190, 209
Kuzmin A. D., Dakesamanskaya I. M., 1984, Astronomy Letters, 10, 854
Kuzmin A. D., Losovsky B. Ya., 1996, A&A, 308, 91
Kuzmin A. D., Izvekova V. A., 1996, Astronomy Letters, 22, 394
Lyne A. G., Manchester R. N., 1988, MNRAS, 234, 447 (LM88)
Radhakrishnan V., Cooke D. J., 1969, ApJ, 3, L225
Rankin J. M., 1993a, ApJ, 405, 285 (R93a)

Rankin J. M., 1993b, ApJS, 85, 145 (R93b)
Ruderman M. A., Sutherland P. G., 1975, ApJ, 196, 51
Wu X. J., Xu W., Rankin J. M., 1992, In: T. H. Hankins, J. M. Rankin, J. A. Gil, eds., IAU Collq. 128, The Magnetospheric Structure and Emission Mechanism of Radio Pulsars., Zielona Góra Poland: IAU, p.172
Wu X. J., Manchester R. N., 1992, In: T. H. Hankins, J. M. Rankin, J. A. Gil eds., IAU Collq.128, The Magnetospheric Structure and Emission Mechanism of Radio Pulsars., Zielona Góra Poland: IAU, p.362
Wu X. J., Yu K. Y., Zhang C. M. et al., 1999, Chinese Physics Letters, 16, 74 (WU99)
Wu X. J., Gil J., 1995, Chin. J. Astron. Astrophys., 19, 156
Wu X. J., Huang Z. K., Xu X. B., 2002, Chin. J. Astron. Astrophys., 454 (Wu02)
Wu X. J., Gao X. Y., Rankin J. M. et al., 1998, AJ, 116, 1984
Xu X. B., Wu X. J., 2002, Science of China, 32, 1134